Neuron, Vol. 46, 731–744, June 2, 2005, Copyright ©2005 by Elsevier Inc. DOI 10.1016/j.neuron.2005.04.024

ATP Released via Gap Junction Hemichannels from the Pigment Epithelium Regulates Neural Retinal Progenitor Proliferation

Rachael A. Pearson,[1,3,*] Nicholas Dale,[2] Enrique Llaudet,[2] and Peter Mobbs[1]
[1]Department of Physiology
University College London
Gower Street
London WC1E 6BT
United Kingdom
[2]Department of Biological Sciences
University of Warwick
Coventry CV4 7AL
United Kingdom

Summary

The retinal pigment epithelium (RPE) plays an essential role in the normal development of the underlying neural retina, but the mechanisms by which this regulation occurs are largely unknown. Ca^{2+} transients, induced by the neurotransmitter ATP acting on purinergic receptors, both increase proliferation and stimulate DNA synthesis in neural retinal progenitor cells. Here, we show that the RPE regulates proliferation in the underlying neural retina by the release of a soluble factor and identify that factor as ATP. Further, we show that this ATP is released by efflux through gap junction connexin 43 hemichannels, the opening of which is evoked by spontaneous elevations of Ca^{2+} in trigger cells in the RPE. This release mechanism is localized within the RPE cells to the membranes facing the neural retina, a location ideally positioned to influence neural retinal development. ATP released from RPE hemichannels speeds both cell division and proliferation in the neural retina.

Introduction

During retinal development, the retinal pigment epithelium (RPE) lies adjacent to the retinal ventricular zone (VZ), the outermost layer of the neural retina where progenitor cells undergo an intense period of repeated cycles of cell division to generate all the neurons and glia of the adult structure. A number of observations suggest that the RPE, together with its unique juxtaposition with the neural retina, is essential for the normal development of the retina. First, early ablation of RPE cells leads to disorganization of the neural retina, the arrest of eye growth, and ultimately reabsorption of the eye. Ablation of RPE cells at later times results in disruption of the laminar structure of the neural retina, failure of vitreous accumulation, and adults that are anophthalmic or microphthalmic (Raymond and Jackson, 1995). Second, in albinism, a disease in which the RPE lacks pigmentation, the neural retina shows developmental defects, including increased cell proliferation and subsequent cell death, a reduction in the rod photoreceptor population, and an underdeveloped central retina (Ilia and Jeffery, 1996; Ilia and Jeffery, 2000). In addition, in albino mice more ganglion cells are born in the early stages of neurogenesis than in the normally pigmented eye (Rachel et al., 2002), though reduced numbers of these cells are present in albino adult animals (Jeffery, 1997).

The RPE thus plays a pivotal role in the regulation of proliferation and differentiation in the underlying neural retina during development, but the mechanisms by which the RPE exerts this control are poorly understood. One potential mechanism for modulating neural retinal progenitor cell proliferation may involve purinergic signaling (Pearson et al., 2002; Sugioka et al., 1996). Exogenously applied adenosine 5′-triphosphate (ATP) acts on neural retinal progenitor cells, via purinergic P2Y receptors, to evoke Ca^{2+} transients and speed their mitosis, an effect that leads to enhanced proliferation and bigger eyes (Pearson et al., 2002). Activation of ATP receptors has similarly been shown to regulate DNA synthesis and proliferation in astrocytes (Neary and Zhu, 1994), neural stem cells (Ryu et al., 2003), Muller cells (Milenkovic et al., 2003), and most recently cortical progenitors (Weissman et al., 2004).

The RPE supports robust Ca^{2+} waves during early development (Pearson et al., 2004). It is possible that these waves are mediated via the release of ATP, as has been demonstrated for the Ca^{2+} waves that occur in glia (Newman, 2001; Cotrina et al., 1998; Guthrie et al., 1999). We therefore considered the hypothesis that ATP, released via Ca^{2+} waves, might be one signal by which the RPE regulates mitosis in the VZ of the neural retina. We show that, under physiological conditions, ATP is released from RPE cells into the subretinal space and acts to enhance both mitosis and proliferation. However, rather than RPE Ca^{2+} waves being the cause of the ATP release, we find that ATP is released by the spontaneous opening of gap junctional hemichannels in "trigger" cells in the RPE. The subsequent diffusion of ATP from these trigger cells leads to both the stimulation of proliferation in the underlying neural retina and the propagation of a Ca^{2+} wave in the RPE.

Results

The RPE Modulates Mitosis in the Underlying Neural Retinal via a Purinergic Mechanism

P2Y receptors are expressed on neural retinal progenitor cells (Pearson et al., 2002; Sugioka et al., 1996), and exogenously applied purinergic agonists and antagonists act via a Ca^{2+}-dependent mechanism to influence both their rate of mitosis and proliferation, leading to changes in eye size (Pearson et al., 2002). Here, we test whether ATP is released from the embryonic RPE via the Ca^{2+} waves that occur spontaneously within this tissue (Pearson et al., 2004) and, if so, whether it could act to regulate the cell cycle in the neural retina. We

*Correspondence: rachael.pearson@ich.ucl.ac.uk
[3]Present address: Developmental Biology Unit, Institute of Child Health, University College London, London WC1N 1EH, United Kingdom.

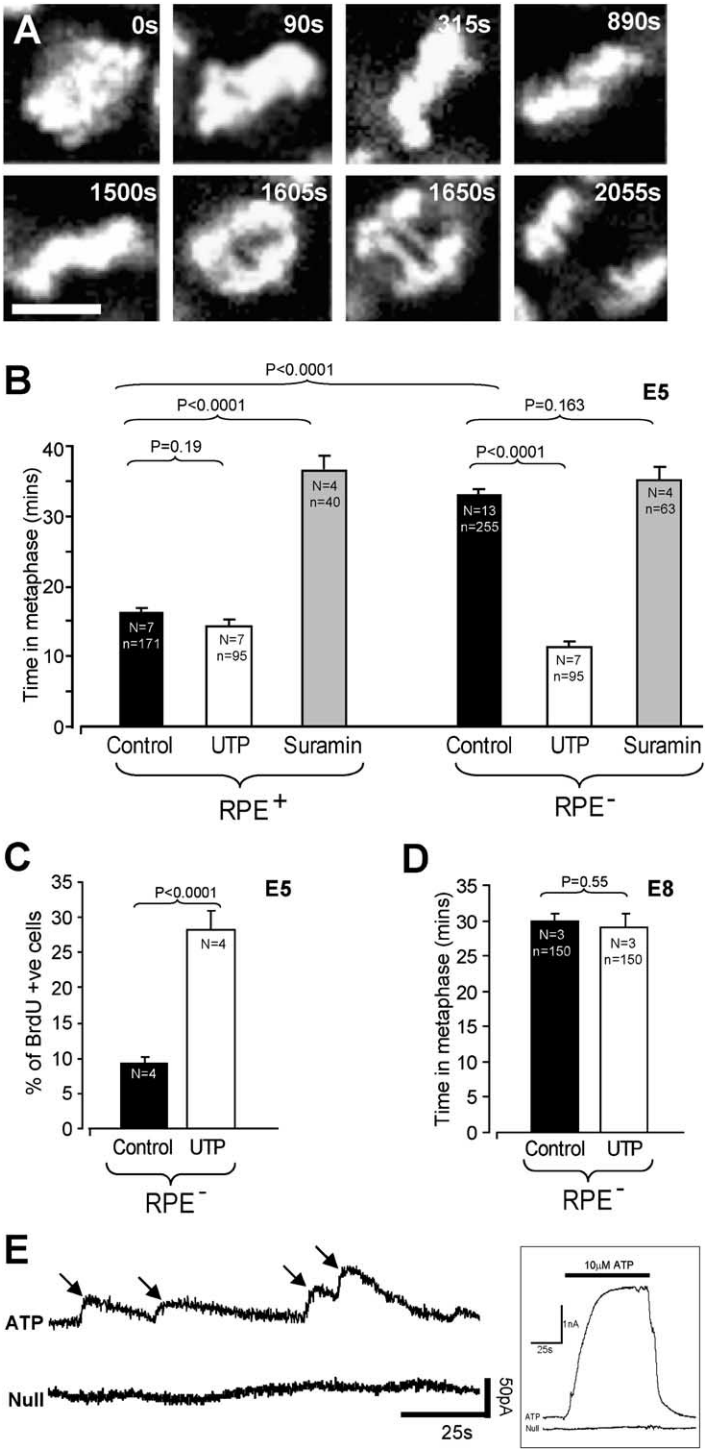

Figure 1. The RPE and ATP Regulate Neural Retinal Mitosis

(A) Example images from a confocal time-lapse series of mitosis in the VZ. The chromatin of the mitotic cell progresses from prophase (0 s), through metaphase (90–1500 s), and into anaphase (1650 s onward). Scale bar, 5 μm. (B) Mitosis in the embryonic neural retinal VZ is faster in the presence of the RPE and purinergic agonists. Histogram shows the time spent in mitosis by progenitor cells in preparations either with the RPE intact (RPE^+, left) (16 ± 1 min), or following its removal (RPE^-, right) (33 ± 1 min). The purinergic agonist UTP restored the rate of mitosis in RPE^- retinas (12 ± 1 min) but had no additional stimulatory effect in RPE^+ preparations (14 ± 1 min). The purinergic antagonist suramin slows the rate of mitosis in RPE^+ preparations (37 ± 2 min) but has little effect on RPE^- preparations (35 ± 2 min). (C) Purinergic agonists increase proliferation in the early embryonic neural retina. Histogram shows the percentage of $BrdU^{+ve}$ cells found following 8 hr exposure to UTP (28% ± 3%), compared with controls (9% ± 1%). (D) The proliferative actions of purinergic agonists decrease with age. Histogram shows the time spent in mitosis by progenitor cells, in the presence or absence of UTP, in the E8 neural retina. N = number of retinas, and n = number of cells investigated. (E) Biosensor recordings of spontaneous ATP release from the retinal face of the isolated RPE (top). Arrows mark individual transient release events that are virtually absent in the null sensor (bottom). (Inset) Application of 10 μM ATP to sensors lifted off tissue. Error bars indicate SEM.

used the DNA label Hoechst 33342 to image progenitor cell mitosis in the VZ of the early embryonic chick neural retina (Figure 1A; see Experimental Procedures and Pearson et al., 2002). Two preparations were used for the experiments described below: (1) the isolated neural retina, from which the RPE had been removed; and (2) a preparation consisting of both the neural retina and the attached RPE.

In isolated neural retinal preparations (RPE^-), progenitor cells spent an average of 33 ± 1 min in mitosis. In contrast, in preparations where the RPE was retained (RPE^+), mitosis proceeded at more than twice this speed (Figure 1B, black bars). However, when RPE^- retinas were exposed to the purinergic P2Y agonist uridine 5′-triphosphate (UTP), the time spent in mitosis was reduced to a period similar to that seen in RPE^+

retinas. UTP had no additional stimulatory effect when applied to preparations retaining their RPE (Figure 1B, white bars). These findings demonstrate that in the absence of the RPE purinergic stimulation of neural retinal progenitor cells is sufficient to restore their rate of progression through mitosis to a level similar to that observed in its presence.

Thus, ATP is able to mimic the presence of the RPE, with respect to maintaining cell division in progenitor cells of the neural retina. To establish whether the stimulatory influence of the RPE similarly involves purinergic receptor activation, we used the P2 receptor antagonist suramin. In RPE^- neural retinas, suramin had little effect, suggesting that there is only a low level of endogenous P2 receptor activation in the neural retina in the absence of the RPE. However, in retinas that retained their RPE (RPE^+) and in which progenitor cells normally proceed rapidly through mitosis, suramin more than doubled the duration taken for cells to divide (Figure 1B, light gray bars), to a time similar to that seen in control RPE^- neural retina preparations. That suramin dramatically slowed cell division in the presence of the RPE, but had little effect in its absence, suggests that the proliferative effect mediated by the RPE involves ATP and the activation of P2 receptors in the neural retina. It is possible that the effects of purinergic antagonists on cell division in the RPE^+ preparations are mediated by acting on the RPE cells rather than the progenitor cells. However, given that ATP mimics the effect of the presence of the RPE in isolated RPE^- neural retinal preparations, that purinergic antagonists had little further effect on division in the isolated neural retina, and that P2Y receptors have previously been shown to be expressed on retinal progenitors (Pearson et al., 2002; Sugioka et al., 1996), the most parsimonious explanation is that the actions of purinergic antagonists on cell division in RPE^+ preparations are mediated via blocking P2-Rs on progenitor cells.

We also measured the rate of progression through mitosis in the presence of apyrase, a Ca^{2+}-activated enzyme that catalyses the hydrolysis of nucleoside di- and triphosphates. Apyrase markedly decreased the mitotic activity of neural retinal progenitor cells, preventing the majority of cells from progressing through mitosis. We were, therefore, also unable to measure the rate of cell division in these preparations. This effect was seen in both RPE^+ and RPE^- retinas. The reasons for such a significant effect in both RPE^+ and RPE^- retinas are not clear, but it may be that other stages of the cell cycle require purines other than ATP that are also degraded by apyrase. However, the results support the notion that extracellular ATP is necessary for normal progression of mitosis in the neural retina.

While purinergic agonists speed progenitor cell division, this may not necessarily be reflected by an increase in proliferation. To test this possibility, isolated RPE^- neural retinas were exposed to 5-bromo-2′-deoxy-uridine (BrdU), which labels dividing cells, in the presence or absence of purinergic agonists. Retinas were then analyzed using confocal microscopy and assessed for the number of $BrdU^{+ve}$ cells. Neural retinas exposed to purinergic agonists showed a 3-fold increase in the level of BrdU incorporation with respect to controls (Figure 1C). Thus, the stimulatory effect of ATP on cell division is reflected in an increased level of proliferation, a conclusion supported by previous findings in which the application of ATP led to increased numbers of dividing cells, larger eyes (Pearson et al., 2002), and an increased rate of DNA synthesis (Sugioka et al., 1999).

In the CNS, cell cycle time usually increases as the tissue matures. This lengthening of the cell cycle could be influenced by the purinergic signaling mechanism described above. Consistent with this, we found that, later in development (E8), UTP was no longer able to speed up mitosis in the RPE^- neural retina (29 ± 2 min in the presence of UTP compared with 30 ± 1 min in controls; N = 3 retinas, n = 150 cells for each; p = 0.55; Figure 1D). Further, we and others have shown that purinergic-induced changes in Ca^{2+} are prevalent early in retinal development (Pearson et al., 2002; Sugioka et al., 1996) but decline between E4 and E6 and are absent by E8 (Sugioka et al., 1996; R.A.P., unpublished data). Sugioka et al. (1999) have shown that P2 receptor-mediated stimulation of DNA synthesis in retinal progenitor cells declines in an age-dependent manner. Cell cycle lengthening thus appears to be correlated with a decrease in the sensitivity of neural retinal progenitor cells to ATP.

Direct Measurement Shows that ATP Is Released from the Retinal Face of the RPE

To test directly whether ATP is released by the RPE, we used ATP-sensitive biosensors. As a control in each experiment, null electrodes that detect nonspecific electroactive substances, but not ATP, were also used. Events occurring on the ATP sensor, but not on the null, provide a measure of the ATP released (see Experimental Procedures; Llaudet et al., 2003; Gourine et al., 2005). The sensing surface of the ATP and null sensors were laid gently on isolated RPE preparations, from which the underlying neural retina had been removed. Transient signals, having a fast rise time (T_{50} = 1.4 ± 0.1 s) followed by a slow decay (T_{50} = 21.6 ± 0.5 s; data taken from N = 13 RPEs and >1000 transients) (Figure 1E), were recorded from the retinal face of the RPE. They occurred spontaneously at a frequency of 11 events/10 min in an area of $\sim 42 \times 10^3$ μm^2 (see Experimental Procedures). These real-time measurements show that ATP is not tonically released but rather occurs as random and transient events. Thus, the embryonic RPE spontaneously releases ATP into the subretinal space, immediately adjacent to where progenitor cells are dividing in the VZ of the neural retina.

Spontaneous Ca^{2+} Waves in the Embryonic RPE Are Associated with the Release of ATP

ATP release has been shown to be associated with Ca^{2+} waves in astrocytes and radial glia. In glial cultures, such waves are thought to propagate through networks of cells either by the diffusion of IP_3 between cells through gap junctions or by the release of ATP, which functions as an extracellular messenger (Guthrie et al., 1999; Newman, 2001). Recently, these apparently parallel mechanisms of wave propagation have been partially explained by the possible involvement of unopposed gap junction hemichannels. In whole gap

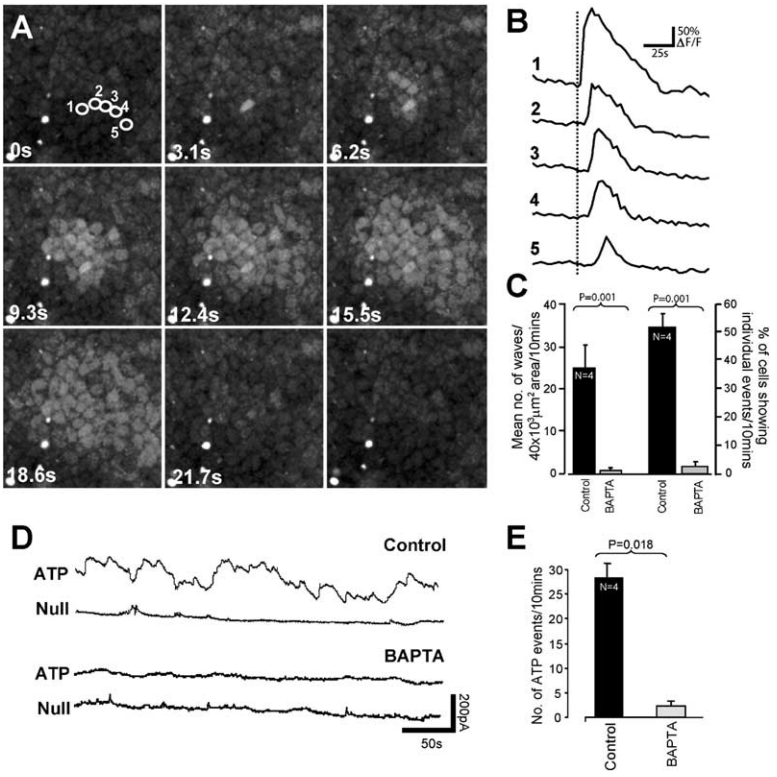

Figure 2. Ca^{2+} Waves Occur Spontaneously in the Embryonic RPE at a Frequency Similar to ATP Release Events

(A) Confocal images from a time series of an isolated RPE loaded with Oregon Green-AM (see Movie S1). A wave was initiated in cell 1 and propagated toward cell 5. Scale bar, 20 μm. (B) Fluorescence changes in cells 1–5 depicted in (A). (C) Preincubation with BAPTA-AM inhibits both Ca^{2+} waves (BAPTA-AM, 1.3 ± 0.9 waves/10 min/42 × 10^3 μm^2 field of view versus 27.3 ± 7.0 waves in controls; left) and spontaneous activity occurring in individual cells (2.5% ± 2% cells active/10 min versus 52% ± 4%; right). (D) Biosensor recordings of ATP release in RPE showing that it requires a change in $[Ca^{2+}]_i$. (E) Histogram of the frequency of ATP release events in BAPTA-AM, compared with controls (BAPTA-AM, 2.7 ± 1.2 events/10 min versus 28.3 ± 3.7 in controls). Error bars indicate SEM.

junctions, each of the coupled cells contributes a hemichannel (or connexon), a hexamer of connexin proteins. Exogenously evoked Ca^{2+} waves in astrocytes have been shown to spread by the release of ATP through unopposed gap junction hemichannels (Stout et al., 2002; reviewed in Bennett et al., 2003), although evidence for spontaneous opening of these channels in physiological conditions is limited and equivocal. Since the RPE is strongly gap junction coupled, supports spontaneous Ca^{2+} waves (Pearson et al., 2004), and releases ATP from its retinal surface (see above), we tested the possibility that these Ca^{2+} waves could be the source of ATP release.

Ca^{2+} changes (and the effects of all the pharmacological manipulations described below) were examined in the isolated RPE, in the absence of the underlying neural retina, using confocal microscopy. Spontaneously occurring Ca^{2+} transients in individual cells are common in the embryonic RPE (Pearson et al., 2004); between 5% and 10% of these transients trigger Ca^{2+} waves. RPE Ca^{2+} waves spread concentrically out from a central "trigger" cell, at a speed of 9 ± 1 μm/s. These waves typically invade 10 to 20 cells, covering an area of 500 ± 95 μm^2, and last 13 ± 1 s (Figures 2A and 2B and Movie S1 in the Supplemental Data available with this article online). The waves were randomly spatially distributed and occurred with a frequency of ~20/10 min/42 × 10^3 μm^2 field of view. The Ca^{2+} transients in individual cells and the resulting waves were blocked by the Ca^{2+} chelator BAPTA-AM (Figure 2C). Both the proportion of cells undergoing spontaneous Ca^{2+} transients and wave frequency were reduced by 96% by BAPTA-AM.

The frequency of the Ca^{2+} waves is similar to that of the ATP release events, although slightly higher than the latter. However, the measurements of ATP release events are likely to underestimate their frequency (see Experimental Procedures). Just as BAPTA-AM prevented Ca^{2+} waves, it also reduced the frequency of ATP release, by 91% (Figures 2D and 2E). Thus, ATP is spontaneously released from the retinal face of the RPE at a rate similar to the frequency of Ca^{2+} waves, via a Ca^{2+}-dependent mechanism.

Spontaneous Ca^{2+} Waves in the Embryonic RPE Require Gap Junctions and/or Hemichannels and ATP

Since RPE cells are highly gap junction coupled to one another (Pearson et al., 2004), we examined whether RPE Ca^{2+} waves are mediated intercellularly through gap junctions or extracellularly by ATP.

We investigated the contribution of the intercellular/gap junction pathway between RPE cells to the propagation of RPE Ca^{2+} waves using a range of gap junction blockers (carbenoxolone [CBX]; 18-α-glycyrrhetinic acid [18-α-GA], and retinoic acid [RA]). These three agents act at both gap junctions and hemichannels.

All three gap junction blockers significantly reduced wave frequency (Figure 3A) and the extent of spread of the remaining waves (Figure 3B). Wave frequency was reduced by 91% by CBX, 98% by RA, and 95% by 18-α-GA, and the extent of spread was reduced by more than 60% in each case, such that only cells immediately adjacent to the trigger cell contributed to the attenuated waves. While the three blockers used have actions other than at gap junctions, they all had very similar effects on the propagation of Ca^{2+} waves, mak-

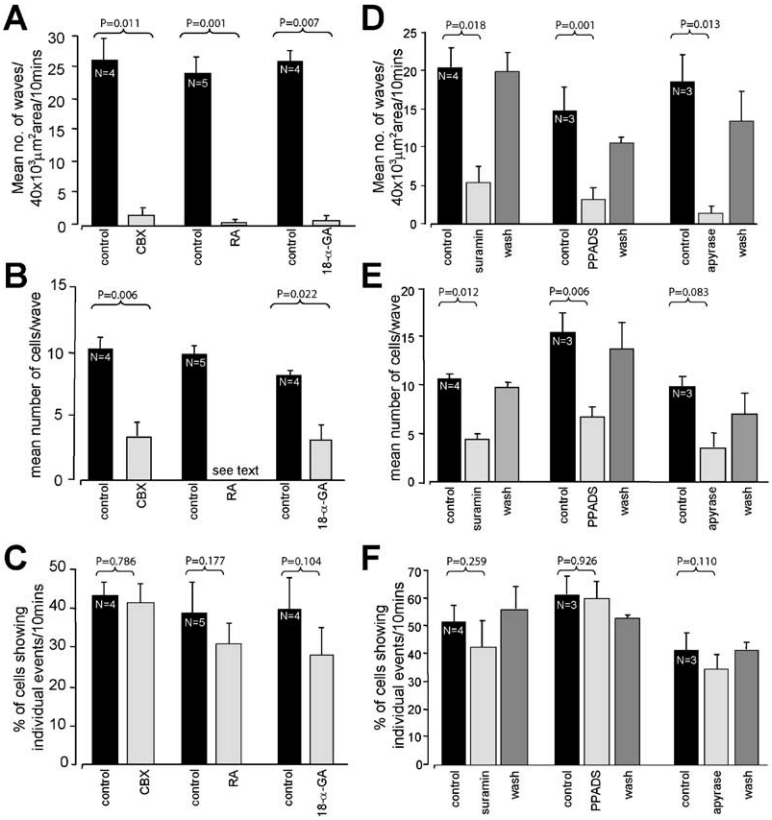

Figure 3. Spontaneous Ca^{2+} Waves in the RPE Involve Gap Junctions and Purinergic Signaling

(A–C) Histograms show effects of CBX, RA, and 18-α-GA, compared with controls, on (A) wave frequency (CBX, 2.3 ± 1.9 waves versus 26.5 ± 3.5 waves in controls; RA, 0.4 ± 0.2 waves versus 23.8 ± 2.9 waves; 18-α-GA, 1.3 ± 0.7 waves versus 26.2 ± 2.0 waves), (B) wave spread (CBX, 3.7 ± 0.3 cells/wave versus 10.2 ± 0.9 in control; 18-α-GA, 3.1 ± 1.2 versus 10.3 ± 0.3 cells; too few waves occurred in the presence of RA to permit statistical analysis), and (C) the proportion of spontaneous Ca^{2+} transients occurring in individual cells (CBX, 42% ± 3% versus 44% ± 3% of cells in controls; RA, 31% ± 3% versus 39% ± 8%; 18-α-GA, 30% ± 6% versus 39% ± 8%) in isolated RPE. (D–F) Histograms show the effects of suramin, PPADS, and apyrase on (D) wave frequency (20.9 ± 2.7, 5.4 ± 2.1, and 20.1 ± 4.0 waves/10 min/ 42 × 10^3 μm^2 in control, suramin, and wash, respectively; 14.8 ± 2.9, 3.2 ± 1.4, and 10.5 ± 0.6 waves in control, PPADS, and wash; 18.3 ± 3.5, 1.5 ± 0.7, and 13.3 ± 5.1 waves in control, apyrase, and wash), (E) wave spread (suramin, 4.5 ± 0.6 cells/wave versus 10.4 ± 0.5 in control; PPADS, 6.7 ± 1.1 versus 15.6 ± 2.1; apyrase, 4.6 ± 1.0 versus 9.9 ± 1.1), and (F) the proportion of spontaneous Ca^{2+} transients occurring in individual cells (suramin, 43% ± 10% versus 52% ± 6% of cells in controls; PPADS, 62% ± 6% versus 63% ± 7%; apyrase, 37% ± 5% versus 42% ± 6%) in isolated RPE. Error bars indicate SEM.

ing it likely that their effects result from their common and well-known actions at gap junctions and/or hemichannels. Furthermore, the Ca^{2+} transients that occur in individual cells, which normally trigger wave spread, continued in the presence of all three blockers and were independent of wave activity (Figure 3C). This indicates that the mechanisms that trigger Ca^{2+} transients in the RPE are unaffected by gap junction blockers.

The involvement of extracellular ATP in the production of RPE Ca^{2+} waves was investigated using the purinergic antagonists suramin and pyridoxal phosphate-6-azo(benzene-2,4-disulfonic acid) tetrasodium salt (PPADS), and the ecto-nucleotidase apyrase. Ca^{2+} waves were reversibly inhibited by all three reagents: wave frequency was reduced by 74% by suramin, 78% by PPADS, and 92% by apyrase, but recovered following washout of each of the drugs (Figure 3D). The extent of the spread of remaining wave activity was also reduced by more than 50% (Figure 3E). Ca^{2+} transients in individual cells were unaffected by any of these purinergic antagonists (Figure 3F).

The evidence above suggests that ATP release and signaling via both gap junctions and/or gap junction hemichannels and purinergic receptors are important in the production of Ca^{2+} waves in the early RPE.

Gap Junctional Hemichannels Are Present at the RPE-VZ Boundary

The gap junction protein connexin 43 (Cx43) is extensively expressed at the margin between the RPE and the VZ of the neural retina (Pearson et al., 2004). As a first step in determining whether or not gap junction hemichannels could form the route for ATP release during RPE Ca^{2+} waves, we used an antibody (Gap7M) directed at connexin hemichannels to examine the pattern of expression of hemichannels in the embryonic retina. Gap7M binds to a region on the first external loop of the connexin, which is only exposed on unopposed gap junction hemichannels and so does not bind to complete gap junctions (Becker et al., 1995). Labeling revealed gap junction hemichannel immunoreactivity that was largely restricted to the RPE (Figure 4A), with only sparse labeling found in the neural retina. Furthermore, the RPE cells are polarized such that hemichannels were concentrated at the junction between the RPE and the VZ (Figure 4A, arrowheads). This location is ideal for the proposed role for hemichannels in the release of ATP from the RPE into the subretinal space to evoke Ca^{2+} waves between RPE cells and modulate mitosis in the neural retina. Staining was absent from controls in which the primary antibody was omitted (Figure 4B).

Ca^{2+} Waves in the RPE Are Mediated by Functional Hemichannels

We next tested whether the hemichannels found in the embryonic RPE are functional. The open probability of gap junction hemichannels is low at normal extracellular Ca^{2+} concentrations. However, hemichannels will open when extracellular Ca^{2+} is reduced (DeVries and

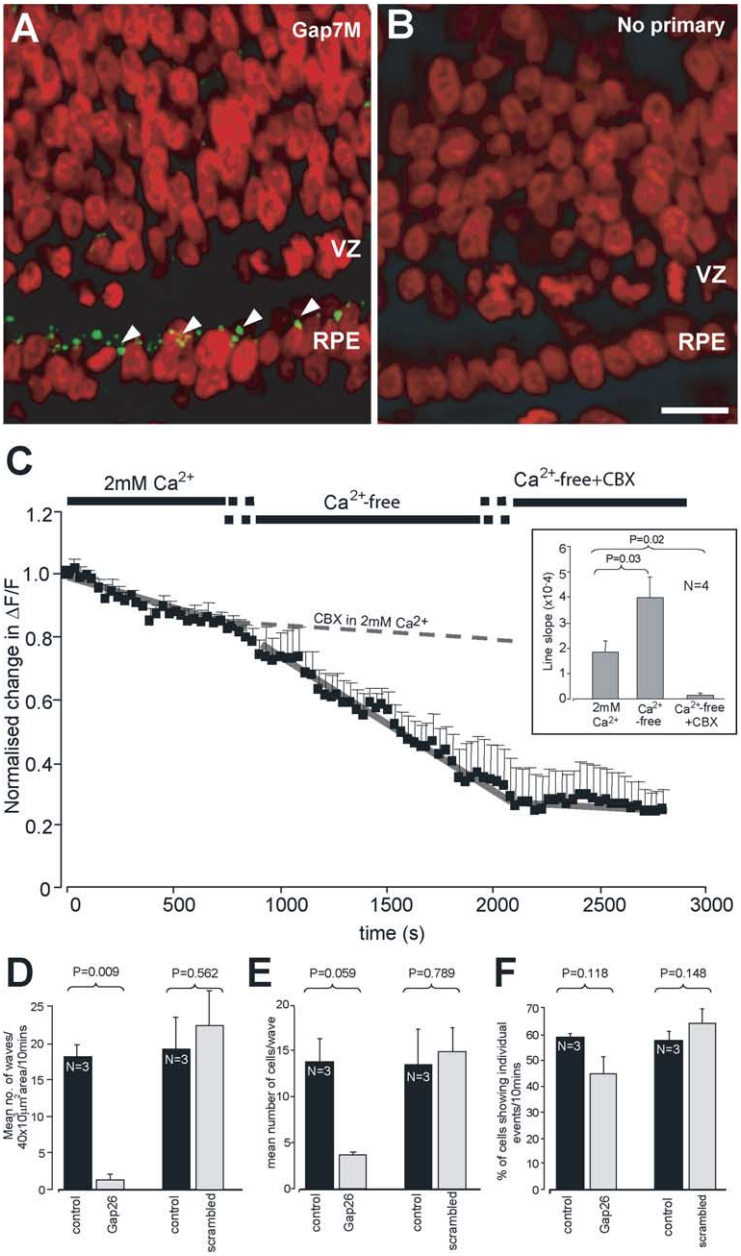

Figure 4. Functional Gap Junction Hemichannels Are Present at the Interface between the RPE and the Neural Retina and Necessary for RPE Ca^{2+} Wave Initiation

(A) Projection of five confocal sections taken at 1 μm intervals through a retina that has been labeled with Hoechst 33342 (pseudocolored red) and Alexa 488-tagged Gap7M (green), an antibody that labels hemichannels. Gap7M staining is highest at the interface between the RPE and neural retina (arrowheads). (B) Control staining in which the primary antibody was omitted. Scale bar, 10 μm. (C) Hemichannel-mediated dye efflux in isolated RPE. Graph shows the average rate of dye efflux in 2 mM Ca^{2+}-containing Krebs, Ca^{2+}-free Krebs, and Ca^{2+}-free Krebs + CBX from Alexa 488-loaded preparations. Dotted line shows average rate of efflux when CBX is added to 2 mM Ca^{2+}-containing Krebs. (Inset) Histogram of the mean slope of fluorescence decay in each of the above conditions. (D–F) Histograms show effects of the hemichannel blocker Gap26 and a scrambled control peptide on (D) wave frequency (Gap26, 1.3 ± 0.9 waves versus 18.1 ± 1.7 waves/10 min/42 × 10^3 μm^2 field of view in controls; scrambled, 22.7 ± 3.9 waves versus 19.3 ± 4.3 waves), (E) wave spread (Gap26, 3.7 ± 0.2 cells/wave versus 13.7 ± 2.6 in control; scrambled, 14.8 ± 2.6 versus 13.4 ± 3.7 cells), and (F) the proportion of spontaneous Ca^{2+} transients occurring in individual cells (Gap26, 45% ± 6% versus 59% ± 9% of cells in controls; scrambled, 64% ± 6% versus 58% ± 3%) in isolated RPE. Error bars indicate SEM.

Schwartz, 1992; Stout and Charles, 2003) and allow passage of many small molecules, including low-molecular weight dyes (Li et al., 1996; Hofer and Dermietzel, 1998). We found that removal of extracellular Ca^{2+} led to the rapid loading of RPE cells with Alexa 488 (MW 570). This loading was reduced by preincubation with CBX. However, gap junction blockers such as CBX act on both whole gap junctions and hemichannels. We therefore employed a connexin mimetic peptide, Gap26, which specifically blocks hemichannels by mimicking a 13 amino acid sequence (VCYDKSFPIS HVR) on the first extracellular loop of Cx43 but does not affect coupled gap junctions (see Experimental Procedures and Braet et al., 2003). Alexa 488 loading was reduced by Gap26, indicating that dye loading in Ca^{2+}-free solutions occurs through the opening of hemichannels. Increasing gap junction hemichannel open probability should also cause a loss of dye from preloaded cells; exposing RPE preloaded with Alexa 488 to a Ca^{2+}-free solution doubled the rate of dye loss (Figure 4C, inset). This loss could be prevented by application of CBX, in either Ca^{2+}-free (Figure 4C) or 2 mM Ca^{2+} solution (dashed line, Figure 4C).

We used Gap26 to test whether hemichannels in the RPE are involved in Ca^{2+} wave production. RPE Ca^{2+} wave activity was reduced by 94% following incubation with Gap26, but a scrambled version of the peptide (PSFDSRHCIVKYV) had no effect (Figure 4D). Similarly, the extent of spread of remaining wave activity was reduced by 73% by Gap26 but remained constant in the

presence of scrambled peptide (Figure 4E). The frequency of Ca^{2+} transients in individual RPE cells was not significantly affected by Gap26 or the scrambled peptide (Figure 4F). Neither CBX nor Gap26 had any effect on the ability of RPE cells to respond to UTP; 88% ± 1% cells showed an above criterion change in Ca^{2+} in response to UTP in controls, 86% ± 1% cells in CBX, and 81% ± 3% with Gap26 (N = 3, n = 150 for each), confirming that these agents' effects on Ca^{2+} waves were not due to a nonspecific action on any cascade downstream from ATP release.

Spontaneous ATP Release in the Embryonic RPE Requires Functional Hemichannels

As ATP is released from the RPE via transient events that occur at a frequency similar to that of spontaneous Ca^{2+} waves, we tested whether this results from the opening of gap junction hemichannels during wave initiation, using preparations of the isolated RPE. The removal of extracellular Ca^{2+} increases the open probability of hemichannels (see above); it also causes a large increase in signal at both the ATP and the null sensors. The signal on the null electrode in Ca^{2+}-free media results from the release of unknown electroactive species under these conditions. In the absence of extracellular Ca^{2+}, individual transient increases in ATP were not seen, an effect which may result from a hemichannel open probability of near to 1.0. However, the ATP signal was consistently and significantly larger than the null (333 ± 46 pA larger than null peak amplitude; N = 9; p = 0.0001). These changes were only seen when the sensors were in contact with the tissue; Ca^{2+}-free Krebs alone had no effect on the sensors (see Figure S1). This signal was prevented by preincubation with Gap26 (5 ± 8 pA smaller than null peak amplitude; N = 3), suggesting that, in Ca^{2+}-free solutions, ATP is released through an increase in gap junction hemichannel open probability.

We next tested hemichannel involvement in ATP release at physiological Ca^{2+} concentrations (1 mM extracellular [Ca^{2+}]). Under these conditions, spontaneous ATP transients were inhibited both by the gap junction/hemichannel blocker CBX (Figures 5A and 5B) and by the hemichannel-specific blocker Gap26 (Figures 5C and 5D). The frequency of events was reduced by 75% and 92%, respectively, while the scrambled control peptide had no effect (Figures 5E and 5F). These results demonstrate that spontaneous release of ATP from the RPE is, like the propagation of Ca^{2+} waves, dependent upon the opening of gap junction hemichannels. To our knowledge, this is the first time that individual ATP release events resulting from the gating of hemichannels have been resolved.

ATP Release through Hemichannels Is Not ATP Dependent

In glial cells, Ca^{2+} waves may propagate in part by the release of ATP via an ATP-dependent mechanism (Ballerini et al., 1996; Anderson et al., 2004), implying that ATP release would be sensitive to purinergic antagonists. However, we found that, in contrast to their inhibitory effect on Ca^{2+} wave propagation, purinergic antagonists had no effect on the frequency of ATP transients (Figures 5G and 5H). This difference in the sensitivity of ATP release and Ca^{2+} waves to blockade of P2 receptors, and our observation that BAPTA-AM prevents ATP release, show that transient increases of Ca^{2+} in trigger cells, but not Ca^{2+} waves themselves, are necessary for release of ATP, i.e., ATP-induced ATP release is not involved in the propagation of RPE Ca^{2+} waves. Rather, it is likely that it is the release of ATP through hemichannels opened in trigger cells alone that causes the Ca^{2+} waves, via passive diffusion to P2Y receptors present in surrounding RPE cells. Consistent with this, the free diffusion coefficient for ATP in physiological solution at 37°C is 0.53×10^{-9} m^2s^{-1}, which would lead to the spread of the ATP released from a trigger cell over approximately 100 μm in 13 s, compared to Ca^{2+} waves, which spread over about 50 μm in the same time (the average duration of RPE Ca^{2+} waves). While the size of the Ca^{2+} waves is more restricted than the calculated spread of ATP, the latter is likely to be an overestimate, given the likely presence of factors such as extracellular matrix proteins and ATPases, which would limit the free diffusion of ATP.

RPE Ca^{2+} Waves Are Initiated by the Ca^{2+}-Dependent Opening of Hemichannels in Trigger Cells

To further determine whether the trigger cell alone is responsible for the hemichannel-mediated release of ATP, we used propidium iodide (PI; 562 Da) to monitor the opening of hemichannels (Arcuino et al., 2002) during wave propagation. PI is a gap junction-permeant molecule that fluoresces when it binds DNA but, due to its charge, is unable to cross cell plasma membranes. We found that, in 87% of spontaneous Ca^{2+} waves, only the trigger cell became labeled with PI (Figures 6A and 6B; see Movie S2), while none of the surrounding cells involved in the wave became labeled. Only 0.5% of cells showing a spontaneous Ca^{2+} transient that did not then subsequently spread as a wave became labeled with PI (Figure 6B). Thus, only Ca^{2+} transients that lead to waves are associated with PI uptake.

Three observations show that the increase in the permeability of the trigger cell membrane detected by PI influx was transient and did not result from a loss of membrane integrity. First, cells observed to trigger Ca^{2+} waves in the RPE excluded PI if the indicator was added after wave initiation (N = 3 retinas, n = 21 waves). Second, some trigger cells initiated more than one wave within the recording period. When this occurred, the second rise in Ca^{2+} led to a further increase in PI fluorescence (Figure 6C). Third, $[Ca^{2+}]_i$ levels in trigger cells return to normal following a transient (Figure 6C).

Prior incubation of RPE tissue with the hemichannel blocker Gap26 prevented both wave initiation and PI uptake (0 PI^{+ve} cells/10 min/42×10^3 μm^2) (Figure 6B), while the scrambled peptide had no effect on wave frequency, and 90% of trigger cells were PI^{+ve} (Figure 6B). That Gap26 prevents PI influx indicates that, when trigger cells initiate Ca^{2+} waves, they show a transient increase in gap junction hemichannel open probability. Since only the trigger cell and none of the other cells involved in the Ca^{2+} wave labeled with PI, it is likely that the ATP required for Ca^{2+} wave propagation comes solely from the opening of hemichannels in the trigger

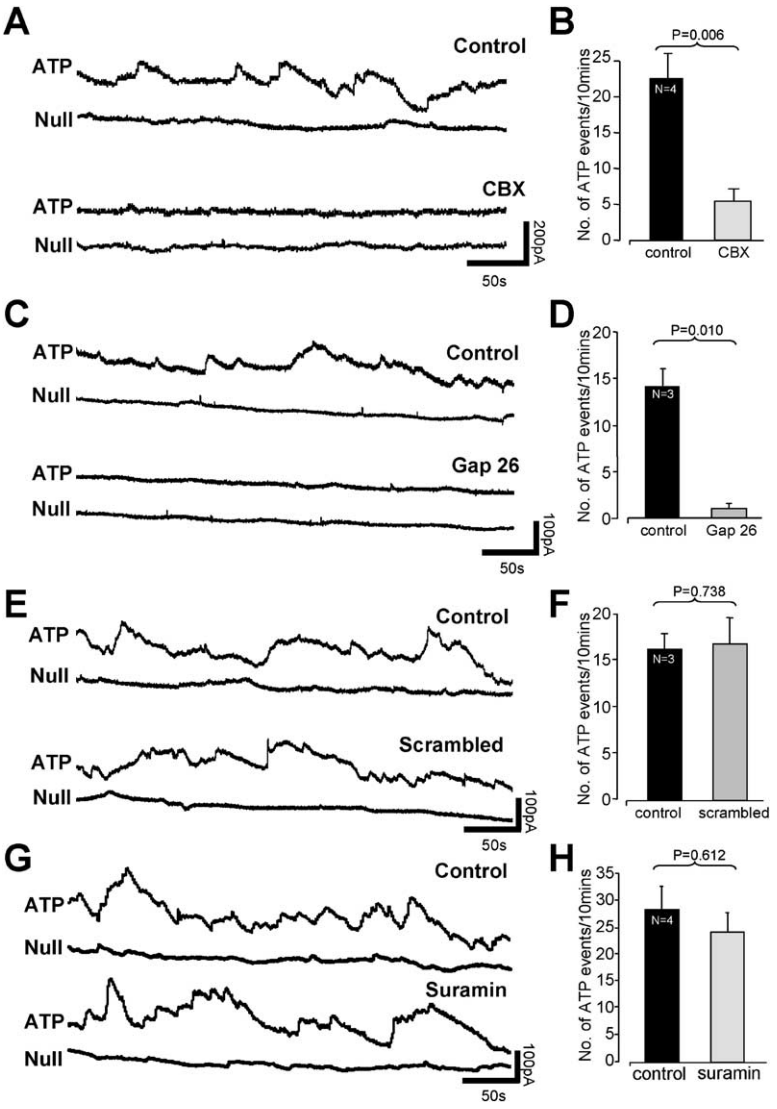

Figure 5. Spontaneous ATP Release from the RPE Requires Gap Junction Hemichannels but Does Not Involve ATP-Induced ATP Release

(A–F) ATP release is blocked by gap junction and hemichannel blockers. ATP release is virtually abolished following exposure to (A) CBX and (C) Gap26 but is unaffected by (E) scrambled peptide control. (B, D, and F) Histograms of the frequency of ATP release events in CBX (5.6 ± 1.6 events/10 min versus 22.6 ± 3.4 in controls), Gap26 (1.0 ± 0.5 events/10 min versus 14.2 ± 1.7), and scrambled peptide (16.8 ± 2.9 events/10 min versus 16.2 ± 1.7 events/10 min), compared with controls. (G and H) ATP release is unaffected by purinergic blockers. (G) ATP release is maintained in the presence of suramin. (H) Histogram of the effects of suramin on the frequency of ATP release events (24.3 ± 3.6 events/10 min in suramin versus 28.4 ± 4.4 in controls). Error bars indicate SEM.

cell alone. We cannot rule out the possibility that ATP released from trigger cells is amplified by release from neighboring cells via a gap junction hemichannel-independent mechanism. However, that purinergic antagonists were able to block Ca^{2+} waves but had no effect on ATP release (see above) indicates that ATP-induced ATP release is not involved. The signaling pathway that leads to the opening of hemichannels in the trigger cell is currently unknown but must involve changes in $[Ca^{2+}]_i$.

The RPE Modulates Mitosis in the Neural Retinal via the Release of ATP through Gap Junction Hemichannels

Based on our demonstration that ATP derived from the RPE is required for cell division in the neural retina to proceed at its normal rate and that ATP is released from the RPE via hemichannels, blockade of hemichannels would be predicted to slow cell division in the neural retinal. We therefore tested the effect of Gap26 on the rate of mitosis in the neural retina. As before, two preparations were used for these experiments: the isolated neural retina, without RPE (RPE^-), or a preparation of the neural retina with the RPE attached (RPE^+). In RPE^+ preparations incubated in the scrambled peptide control, progenitor cells spent an average of 11 ± 1 min in mitosis, a time very similar to that in RPE^+ controls (Figure 7, right; compare with Figure 1B, black bar, left). In contrast, mitosis in RPE^+ preparations exposed to Gap26 was slowed to 30 ± 2 min, a rate close that observed in isolated RPE^- neural retina controls (Figure 7, left; compare with Figure 1B, black bar, right). Conversely, Gap26 had little effect on mitosis in preparations in which the RPE was removed; mitosis proceeded at a rate similar to that seen in both RPE^+ preparations in the presence of the scrambled peptide and in RPE^- controls. The low level of hemichannel immunoreactivity in the neural retina (Figure 4A), together with the finding that Gap26 had no effect on mitosis in isolated RPE^- neural retinal preparations, indicates that hemichannel-mediated ATP activity in the neural retina (as opposed to the RPE) is unlikely to be a significant

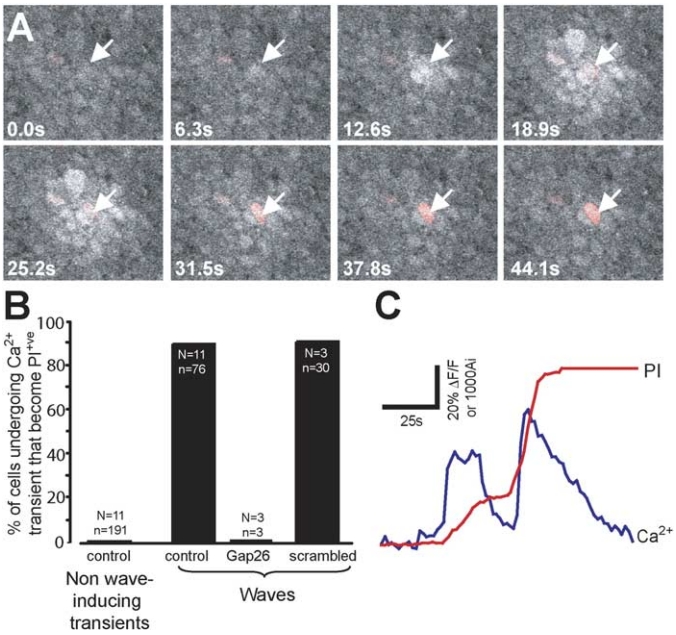

Figure 6. Propidium Iodide Is Only Taken up by the Trigger Cells that Initiate RPE Ca^{2+} Waves

(A) Confocal images from a time series showing propidium iodide (PI) (red) uptake in the cell initiating a Ca^{2+} wave (arrow; see Movie S2).

(B) Histogram showing (left) the percentage of cells that were PI^{+ve} following individual spontaneous Ca^{2+} transients that did *not* evoke waves and (right) the percentage of waves that contained a PI^{+ve} trigger cell in controls and in the presence of Gap26 or scrambled peptide.

(C) Trace showing the change in Ca^{2+} indicator (blue) and PI (red) fluorescence in a single trigger cell. The cell initiated two waves, and each is associated with an increase in PI fluorescence.

regulatory mechanism of retinal progenitor cell mitosis. Consistent with this notion, direct measurement of ATP in the isolated neural retina revealed only very infrequent ATP events (0.3 ± 0.1 events/10 min/42 × 10^3 μm^2), although a hemichannel-independent, tonic release of ATP cannot be ruled out.

We conclude that ATP, spontaneously released from the RPE via gap junction hemichannels, is necessary for maintaining normal rates of progenitor cell division in the underlying neural retina.

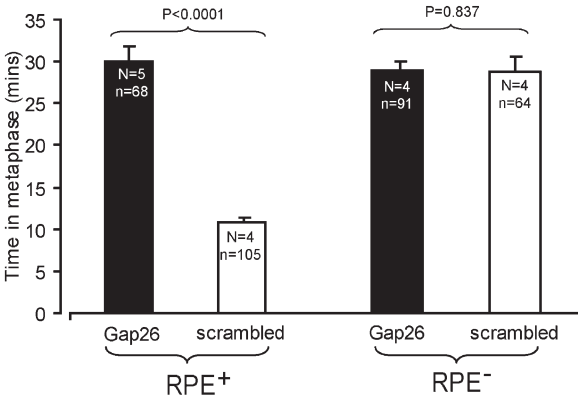

Figure 7. Hemichannel-Mediated ATP Release from the Embryonic RPE Is Necessary for Normal Rates of Mitosis in the Neural Retina

The hemichannel blocker Gap26 slows mitosis in the neural retina of RPE^+ preparations. Histogram shows the time spent in metaphase by neural retinal progenitor cells in RPE^+ (left) or RPE^- (right) preparations in the presence of either Gap26 or the scrambled peptide. Gap26 significantly slowed mitosis in RPE^+ preparations (30 ± 2 min in Gap26, 11 ± 1 min in scrambled peptide) but had no effect on mitosis in RPE^- retinas (29 ± 1 min), compared with the scrambled peptide (29 ± 2 min). Error bars indicate SEM.

Discussion

The RPE is essential for the normal development of the underlying neural retina (e.g., Ilia and Jeffery, 1996; Ilia and Jeffery, 2000; Jeffery, 1997; Rachel et al., 2002; Raymond and Jackson, 1995), but little is known about the regulatory mechanisms involved. Here, we present evidence for a purinergic signaling mechanism by which the early embryonic RPE modulates the proliferation of neural retinal progenitors. Spontaneous Ca^{2+} transients in trigger cells in the RPE lead to the opening of Cx43 gap junction hemichannels located at the retinal face of RPE cells. ATP released via these open hemichannels subsequently diffuses both into the VZ of the underlying neural retina, where it acts on P2Y receptors on neural progenitor cells, stimulating mitosis and proliferation, and to neighboring RPE cells, where it similarly activates purinergic receptors, evoking a rise in $[Ca^{2+}]_i$ and the propagation of a Ca^{2+} wave (Figure 8). RPE-derived ATP appears to be necessary to maintain normal mitosis in the neural retina during early development. To our knowledge, this is the first demonstration of an ATP-dependent signaling mechanism between the RPE and the neural retina. Further, our data provide both strong evidence for the spontaneous activation of gap junction hemichannels under physiological conditions and a detailed characterization of their involvement in the release of purines. Taken together with reports of hemichannels in other cell types, our data indicate that gap junction hemichannel-mediated purinergic signaling should be considered as an important mechanism of cell-cell signaling.

Purinergic Regulation of Proliferation in the Neural Retina by the RPE

Our data show that ATP released from the RPE stimulates progenitor cell division in the underlying neural

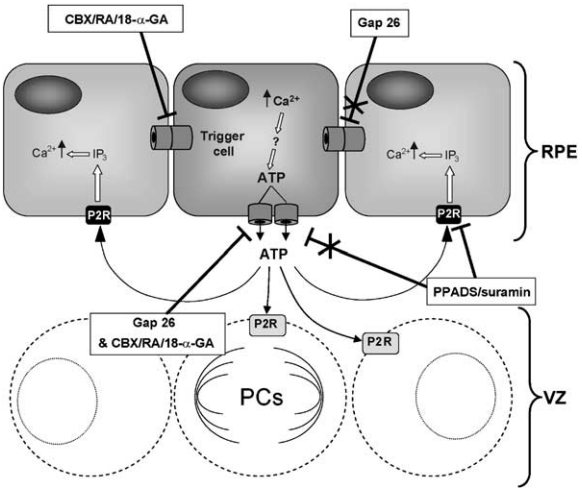

Figure 8. ATP Release from the Embryonic RPE

Diagram showing the proposed mechanism of ATP release and wave propagation in the embryonic RPE. A spontaneous rise in $[Ca^{2+}]_i$ in a trigger cell evokes the opening of Cx43 hemichannels, via an as yet unknown downstream pathway. ATP is released through the hemichannels and diffuses to (1) neighboring RPE cells, where it produces an increase in $[Ca^{2+}]_i$ via P2 receptors, and (2) dividing progenitor cells in the adjacent neural retina, where it acts to increase the speed of mitosis, again acting via P2 receptors (see Pearson et al., 2002).

retina during the proliferative period of development. Cell division is faster in the presence of the RPE than when it is absent, and the mitogenic effect of the RPE can be mimicked by extracellular ATP and prevented by purinergic antagonists. Application of P2Y antagonists proportionately slow the rate of mitosis within the progenitor cell population of the neural retina to a much greater extent in the presence of the RPE than when it is absent. Thus, it is likely that the RPE represents a major source of the ATP necessary for cell division in the neural retina to occur at its normal rate.

ATP has been shown to have proliferative effects on both astrocytic (Rathbone et al., 1992; Franke et al., 1999; Neary et al., 1999; Ciccarelli et al., 2000) and radial glia (Weissman et al., 2004) and neural stem cells (Ryu et al., 2003). One way in which ATP might modulate proliferation is by changes in progenitor cell $[Ca^{2+}]_i$. Changes in Ca^{2+} are required for progression through mitosis and other stages of the cell cycle (Berridge, 1995). In astrocytic cultures, ATP-induced proliferation is accompanied by Ca^{2+} oscillations (Morita et al., 2003), the duration of which similarly regulates proliferation in retinal Muller glia (Moll et al., 2002), which can act as progenitors in the adult retina following injury (Fischer and Reh, 2001; Fischer and Reh, 2003). Consistent with these findings, retinal progenitor cells undergo P2Y receptor-mediated changes in Ca^{2+} (Sugioka et al., 1996; Pearson et al., 2002), and the mitogenic effect of extracellular ATP is mediated via a Ca^{2+}-dependent mechanism (Pearson et al., 2002).

Weissman et al. (2004) have demonstrated that radial glial proliferation is modulated by the propagation of ATP-induced Ca^{2+} waves between glia. A similar mechanism may exist in the proliferating retina, since spontaneous Ca^{2+} waves are also a common feature of the retinal VZ (Catsicas et al., 1998; Pearson et al., 2002; Pearson et al., 2004; Syed et al., 2004). It is possible that ATP-evoked changes in $[Ca^{2+}]_i$ in retinal progenitors could subsequently spread as waves to neighboring cells via gap junctions, given that retinal progenitor cells, like those in the cortex (LoTurco and Kriegstein, 1991; Bittman et al., 1997), are extensively gap junction-coupled to one another (Pearson et al., 2004). However, in contrast to cortical radial glia, it seems unlikely that the release of ATP from retinal progenitor cells themselves is important in maintaining normal rates of proliferation; real-time measurements suggest that ATP release within the neural retina is low, and both purinergic antagonists and the hemichannel blocker Gap26 had little effect on mitosis in the absence of the RPE.

Hemichannel-Mediated ATP Release from the Embryonic RPE

Here, we present strong evidence for the release of ATP via gap junction hemichannels under physiological conditions. Gap junctions are formed by the apposition of two hemichannels from adjacent cells. Unopposed hemichannels provide a channel between the inside of a cell and the extracellular space. There is increasing evidence to suggest that ATP and other small molecules can be released via hemichannel opening (reviewed in Bennett et al., 2003). In cultured astrocytes, ATP is released in response to reduced extracellular Ca^{2+}, stimulation with quinine, mechanical stimuli (Stout et al., 2002; Arcuino et al., 2002), and metabolic inhibition (Contreras et al., 2002). The hemichannels in astrocytes are comprised of Cx43, the same connexin as that found in the embryonic RPE (Pearson et al., 2004). However, until now the evidence for the opening of hemichannels under physiological, as opposed to evoked, conditions has been sparse. Further, many of the pharmacological tools used to assess hemichannel opening have actions other than at hemichannels.

Consistent with a hemichannel-mediated release mechanism, antibodies directed at an external loop on the connexin, which is only accessible in hemichannels since it is hidden in the complete junction (Becker et al., 1995), reveal abundant gap junction hemichannels at the retinal face of the RPE, a position ideal for their proposed role in the release of ATP into the subretinal space. In the retina, Gap26 is an effective blocker of Cx43 gap junction hemichannels, but inactive at complete Cx43 gap junctions (see Experimental Procedures). Crucially, we show that the specific hemichannel-blocking peptide Gap26, as well as conventional gap junction blockers, prevents the release of ATP. A scrambled version of Gap26 had no effect on the release of ATP. Further, lowering extracellular Ca^{2+}, an action known to cause hemichannel opening, causes increased ATP release from, and uptake of a small dye (Alexa 488) into, RPE cells. Each of these effects could be prevented by Gap26 or by raising extracellular Ca^{2+}. Taken together, these results demonstrate that the embryonic RPE expresses Cx43 hemichannels in a location appropriate for the release of ATP into the subretinal space and that these chan-

nels open spontaneously under physiological conditions to mediate the release of ATP. Given the large and nonspecific nature of the Cx43 hemichannel conductance, hemichannel opening in normal $[Ca^{2+}]_o$ might be expected to lead to cell death (Cusato et al., 2003). However, trigger cells in the RPE and other cells that signal via hemichannels may be protected from any deleterious effects through their strong gap junctional coupling to neighboring cells (Andrade-Rozental et al., 2000; Pearson et al., 2004).

Ca^{2+} Waves in the Embryonic RPE

In astrocytes and glia, Ca^{2+} waves have been associated with the release of ATP via hemichannels (reviewed by Bennett et al., 2003). Since Ca^{2+} waves are a common feature of the embryonic RPE (Pearson et al., 2004), we reasoned that these waves could be the source of ATP release. Spontaneous Ca^{2+} transients in RPE cells can trigger the occurrence of Ca^{2+} waves. Consistent with a Ca^{2+}-dependent release mechanism, BAPTA-AM prevents both RPE Ca^{2+} transients and waves and the release of ATP, indicating that ATP release is dependent upon the preceding Ca^{2+} transients in trigger cells, although the mechanism linking these transients to the release of ATP is unknown. The application of any of a panel of conventional gap junction blockers, or the hemichannel blocker Gap26, leads to the inhibition of both Ca^{2+} waves and the release of ATP from the RPE. Similarly, wave spread can be blocked with the purinergic antagonists suramin and PPADS and the ecto-nucleotidase apyrase, thus demonstrating that ATP released from hemichannels is responsible for the propagation of RPE Ca^{2+} waves into surrounding cells. However, the latter maneuvers, designed to prevent ATP's action at P2Y receptors on RPE cells surrounding the trigger cell, have no effect on trigger cell activity or the release of ATP, as demonstrated by Ca^{2+} imaging and biosensor recording, respectively. Thus, endogenous RPE Ca^{2+} waves are most likely evoked by the release of ATP via the opening of unopposed gap junction hemichannels in trigger cells, rather than the diffusion of IP_3 or other second messengers through gap junctions between neighboring cells. Similarly, the trigger cells alone, and not the resulting waves, appear to be responsible for the release of ATP into the subretinal space. Consistent with this, hemichannel opening only occurs in the trigger cell, and not in adjacent cells that take part in the wave, as demonstrated by the uptake of small dye molecules (PI).

Given that Ca^{2+} waves in the RPE appear to be the result, rather than the cause, of ATP release, it is interesting to speculate what their function might be. It is possible that they lead to the release of a mitogenic factor in addition to ATP (Weissman et al., 2004). However, exogenous ATP alone is sufficient to mimic the RPE's ability to enhance cell division in the neural retina. Alternatively, since Ca^{2+} waves like those described here have been shown to pass between the RPE and the neural retina (Pearson et al., 2004), Ca^{2+} waves in the RPE may act to locally synchronize cell cycle events in the underlying neural retina. In the developing cortex, Ca^{2+} waves occur in columnar patches (Peinado et al., 1993; Weissman et al., 2004; Yuste et al., 1995), and the cells that form coupled clusters are clonally related, progressing through the cell cycle in synchrony (Cai et al., 1997). Further studies are required to elucidate the role of Ca^{2+} waves and determine whether they fulfill a role similar to that in the cortex.

The evidence presented here demonstrates a strong association between the release of ATP and the proliferation of neural progenitor cells. Understanding the mechanisms that lead to hemichannel-mediated ATP release may be key to understanding diseases that affect neuronal and astrocyte cell number and be important in developing future strategies that employ stem or retinal progenitor cells in therapeutic interventions.

Experimental Procedures

Retinas

E5 (unless otherwise stated) White Leghorn or Rhode Island Red embryos were killed by decapitation, and their eyes were removed and freed from the overlying sclera. Retinas were dissected at room temperature (RT) in Krebs solution containing the following: 100 mM NaCl, 30 mM $NaHCO_3$, 6 mM KCl, 3 mM NaH_2PO_4, 1 mM $MgCl_2$, 1 mM $CaCl_2$ and 20 mM glucose (pH 7.4 by gassing with 5% CO_2/95% O_2). Three preparations were used in the experiments described: (1) the isolated neural retina, from which the RPE had been removed (RPE^-), (2) a preparation consisting of both the neural retina and the attached RPE (RPE^+), and (3) the isolated RPE, from which the underlying neural retina had been removed.

Imaging of Mitosis

Retinas were dissected out either with the RPE intact, or with careful removal of the overlying RPE. Where possible, within-embryo pairs of eyes were used, with one retina serving as a control and the other being used for drug application. The order in which the two retinas (control or drug) were used was alternated between experiments. The second eye was maintained at 36°C with RPE and lens in place until dissection immediately prior to use. Because the RPE has a tendency to separate from the retina over time, it was not always possible to obtain paired data, so results were pooled. Hoechst 33342 (2 μM; Molecular Probes, UK) was added to the bathing solution 10 min prior to use.

Preparations were transferred to the stage of an inverted microscope (LSM510, Zeiss, UK), mounted with the VZ facing the objective and held flat with nylon strands glued to a platinum frame. The tissue was continually superfused with Krebs solution and imaged at 36°C. xy images of the Hoechst-stained chromatin in the VZ were acquired at 15–20 s intervals for 90 min. The effect of drugs on the rate of mitosis was determined by measuring the time spent in metaphase, defined as the time from which condensed chromatin was first seen as a rod-like structure to the first separation of the chromosomes. These transitions were distinct (Adams, 1996; Pearson et al., 2002) and occurred within one to three images. All recordings were analyzed "blind" and offline using Zeiss LSM imaging software (Zeiss, UK).

Cell Proliferation

BrdU (10 mg/ml; Sigma) was added to the culture medium of eyecups cultured for 8 hr. BrdU incorporation was observed by immunohistochemistry. Eyes were fixed in 4% PFA/PBS for 2 hr, transferred to 20% sucrose/PBS for 30 min, and then embedded in OTC and frozen. Cryostat sections (20 μm thick) were cut and affixed to poly-L-lysine-coated slides. Only sections passing through the center of the retina, adjacent to the optic nerve, were processed. Tissue sections were treated with 0.1 M HCl for 30 min at RT, followed by 2 M HCl for 30 min at 37°C and 0.1 M sodium borate for 10 min at RT, before thorough washing with PBS. A blocking solution (0.1% Tween, 1% FCS, 10% BSA in PBS), containing rat anti-BrdU primary antibody (1:100), was applied overnight at 4°C. After being rinsed for 3 × 10 min with PBS, the sections were incubated with a goat anti-rat FITC-tagged secondary antibody (1:50; Jackson Research) for 4 hr at RT. Following a further 3 × 10 min rinse

with PBS containing 2 μM Hoechst 33342, sections were mounted in Citifluor (Citifluor Ltd, UK) underneath a coverslip. Negative controls consisted of sections processed as above but in the absence of primary antibody. Sections were imaged on a confocal microscope. The percentage of $BrdU^{+ve}$ nuclei was determined by counting $BrdU^{+ve}$ cells and $Hoechst^{+ve}$ cells of the corresponding tissue sections. Sections from four independent experiments, each containing at least 300 nuclei, were analyzed for each determination.

ATP Biosensor Measurements

Biosensors for ATP were manufactured utilizing a two-enzyme cascade (glycerol kinase [EC 2.7.1.30] and glycerol-3-phosphate oxidase [EC 1.1.3.21]) trapped within a polymeric matrix deposited around Pt wire (Llaudet et al., 2003; Gourine et al., 2005) etched to a final diameter of 100 μm. The sensor had an exposed length of ~1 mm that was coated with enzymes and thus capable of detecting ATP. ATP sensors maintain a linear response from 0.2 to 50 μM ATP. They are insensitive to adenosine-5′-diphosphate, adenosine, and UTP (Gourine et al., 2005). Two types of sensor were used in the present study: first, null sensors, possessing only the polymeric coating but no enzymes, were used as a control to check whether any nonspecific electroactive species were released from the preparation that could confound the measurements. Second, sensors containing the enzymes were used. Changes occurring on the ATP sensor, but not on the null, gave the specific ATP signal. Sensors were laid on preparations of isolated RPE, side by side, on the surface facing the retina.

Two kinds of ATP sensor were used to detect ATP release: small disk sensors made by cutting 250 μm diameter insulated Pt wire at an angle and coating the cut end with enzymes, and larger cylindrical sensors made by coating 100 μm diameter Pt wire over about 1 mm of its length. The smaller electrodes have an active area of ~49,000 μm^2, and the large electrodes have an area of ~314,000 μm^2. However, in the case of the disk sensors all of the active area is in contact with the tissue, while for the cylindrical sensors we estimate about one-third or less of the coated area of the electrode contacts the tissue. Consistent with this, disk electrodes detected proportionately fewer ATP events (13 ± 2 events/10 min) than the larger electrodes (24 ± 4/10 min). Since the smaller disc electrodes are much harder to fabricate, the larger electrodes were used in most experiments. Both types of sensor were calibrated by measuring the steady current evoked by solutions containing known concentrations of ATP both before and after each experiment. This ensured that the sensitivity of the electrodes remained constant over the lifetime of their use. ATP release was quantified by counting any change in sensor current greater than 10 pA with a rise time of less than 10 s as an "event." This method underestimates the number of release events, since these fuse at higher frequencies. Rise and decay times were defined as the time taken to reach half-maximal signal increase or decrease, respectively (T_{50}). The 10–25 pA currents that appear to correspond to a single release event equate to exposing the entire disk sensors to between 160 and 400 nM ATP, although the ATP released from the retina may not cover such an area, implying a higher ATP concentration.

Experiments were performed to test whether CBX, Gap26, scrambled peptide, suramin, or Ca^{2+}-free Krebs affected the sensitivity of the sensors. Sensors were placed in the recording chamber, without any tissue present, and perfused with normal Krebs. For each drug, the signal evoked by bath perfusion of ATP (10 μM) was recorded both in Krebs containing the appropriate drug and in control Krebs. The sensitivity of the sensors was not affected by CBX, Gap26, scrambled peptide, or zero Ca^{2+} (see Figure S1). Suramin causes a 30% reduction in the sensitivity of the ATP sensor. However, the sensors remained sufficiently sensitive to show that ATP is released from RPE cells in the presence of suramin (see Results).

Ca^{2+} Imaging

Whole-mount RPEs were isolated by careful dissection from the underlying neural retina immediately prior to use. RPE preparations were loaded with Oregon Green BAPTA-AM (10 μM; Molecular Probes) and the dispersant Cremophor-EL (0.03%; Sigma) for 1.5 hr at 36°C, then maintained in gassed Krebs solution at 36°C. Preparations were mounted on the stage of a confocal microscope, as described above.

xy images were acquired at 3–5 s intervals and analyzed offline using Lucida software (Kinetic Imaging Ltd., UK). The mean fluorescence of individual cells was calculated and normalized to its initial value at time 0. Increases in the fluorescence of Oregon Green reflect increases in $[Ca^{2+}]_i$. A change in fluorescence in excess of a criterion level of 10% above baseline was accepted as a response. Spontaneous Ca^{2+} waves were defined as groups of three or more cells undergoing a spatially and temporally cocoordinated increase in $[Ca^{2+}]_i$ above criterion. Spontaneous activity in individual cells was assessed from a random selection of ~50 cells/retina.

Hemichannel Immunohistochemistry

Chick embryo heads were fixed in 4% PFA/PBS for 2 hr, transferred to 20% sucrose/PBS overnight at 4°C, and then embedded in OTC and frozen. Cryostat sections (20 μm thick) were cut and affixed to poly-L-lysine-coated slides. Sections passing through the center of the retina, adjacent to the optic nerve, were processed. A blocking solution (0.1% Triton X-100, 0.1 M l-lysine in PBS), containing polyclonal rabbit anti-Gap7M primary antibody (1:100; kind gift of David Becker, UCL), was applied for 4 hr at RT. After being rinsed for 3 × 10 min with PBS, the sections were incubated with an anti-rabbit Alexa 488-tagged secondary antibody (1:500; Molecular Probes) for 4 hr at RT. Following a further 3 × 10 min rinse with PBS containing 2 μM Hoechst 33342, sections were mounted in Citifluor underneath a coverslip. Negative controls consisted of retinas processed as above but in the absence of primary antibody. Sections were imaged on a confocal microscope.

Dye Efflux and Uptake

Isolated RPE preparations were loaded with Alexa 488 (0.1 mg/ml) for 30 min in Ca^{2+}-free Krebs solution and transferred into Ca^{2+}-containing Krebs without Alexa 488 for 10 min before imaging. Confocal images were acquired at 30 s intervals, and fluorescence intensity was measured for the field of view (42×10^3 μm^2).

Fluorescence Recovery after Photobleaching

Fluorescence recovery after photobleaching (FRAP) was used to establish that Gap26 exerts its effects on GJ hemichannels, rather than whole GJs (Braet et al., 2003), in the chick retina. RPE preparations were loaded with Alexa 488 (0.1 mg/ml; see above) and transferred to a 2 mM Ca^{2+} solution to reduce dye loss through open hemichannels. A small region (~20 μm diameter) of the tissue was photobleached by 10 s exposure to 488 nm light. Recovery of fluorescence was assessed 1000 s after photobleaching. A correction was made for dye fading caused by intermittent exposure to the 488 nm excitation light. This correction was determined by recording the fluorescence change in a similarly sized, nearby region of cells that were not subject to photobleaching but that were exposed to the same levels of 488 nm light used in monitoring recovery of fluorescence.

The time taken for the bleached region to recover from the bleach, as dye reenters from the surrounding unbleached cells via whole GJs, is a measure of GJ coupling. Recovery from photobleaching was followed in the presence of CBX (100 μM), which significantly reduced the extent of FRAP recovery (12.7% ± 3.9% recovery at 1000 s, compared to 84.5% ± 9.2% in controls; N = 4; p = 0.0001), or Gap26 (0.25 mg/ml), which had no significant effect (70.9% ± 9.9% recovery; N = 4; p = 0.345; see Figure S2). The scrambled control peptide was without effect (88.7% ± 3.2% recovery; p = 0.680; Figure S2). This shows that Gap26 blocks only GJ hemichannels, unlike CBX, which blocks both hemichannels and complete GJs.

FRAP was also used to confirm that the purinergic antagonist suramin (100 μM) did not interfere with GJ function (see Figure S2). Suramin had no effect on fluorescence recovery compared with controls (91.4% ± 7.8% recovery; N = 3; p = 0.582).

PI Uptake

Retinas were loaded with Oregon Green BAPTA-AM (as described above) and transferred to a still bath in a temperature-, humidity-, and gas-controlled environment on the stage of a confocal micro-

scope. Immediately prior to recording, the bathing solution was exchanged for one containing 0.5 mM PI (Sigma, UK). The fluorescence of PI was excited using the 543 nm line of the HeNe laser. Dual wavelength (Oregon Green and PI) images were acquired at 1.5–6 s intervals.

Drugs

The following drugs were used: ATP (10 μM), UTP (10 μM), suramin (50 μM), PPADS (30 μM), apyrase (80 U/ml), CBX (100 μM), RA (30 μM), 18-α-GA (50 μM) (all Sigma, UK), BAPTA-AM (Molecular Probes, UK; 50 μM). The mimetic peptides Gap26 (VCYDKSF PISHVR; 0.25 mg/ml) and scrambled Gap26 (PSFDSRHCIVKYV; 0.25 mg/ml) (Severn Biotech) were acetylated and amidated in order to mimic the peptide in situ within the protein. Mimetic peptides were applied for 30 min (Braet et al., 2003), and apyrase and GJ blockers were applied for 10 min prior to recording.

Most GJ blockers require very long washes. Therefore, CBX, 18-α-GA, and RA actions were assessed in control solution and then again in the presence of the blocker. Control experiments demonstrated that there was no rundown in spontaneous Ca^{2+} or ATP activity for >3 hr (data not shown).

Due to the high cost of the compounds involved, some experiments required the use of a nonflowing bath (apyrase, Gap26, and scrambled peptide and PI entry). In control experiments, retinas maintained in still bath in a temperature-, humidity-, and gas-controlled environment continued to generate Ca^{2+} waves of normal size and magnitude or undergo normal cell division for >3 hr.

Statistical Analysis

All quantitative data presented were normally distributed and tested using a paired Student's t test, unless otherwise stated, when an unpaired Student's t test assuming unequal variance was used. The results are mean ± SEM, where N = number of retinas, and where appropriate, n = number of cells investigated.

Supplemental Data

The Supplemental Data that accompany this article include two supplemental figures and two supplemental movies; these files and the conflict of interest statement can be found with this article online at http://www.neuron.org/cgi/content/full/46/5/731/DC1/.

Acknowledgments

We would like to thank David Attwell, Glen Jeffery, and Michael Duchen for their helpful comments on the manuscript; and David Becker for the kind gift of the Gap7M antibody. This work was supported by the Wellcome Trust. The authors have declared a conflict of interest. For details, see the Supplemental Data.

Received: September 27, 2004
Revised: February 28, 2005
Accepted: April 20, 2005
Published: June 1, 2005

References

Adams, R.J. (1996). Metaphase spindles rotate in the neuroepithelium of rat cerebral cortex. J. Neurosci. *16*, 7610–7618.

Anderson, C.M., Bergher, J.P., and Swanson, R.A. (2004). ATP-induced ATP release from astrocytes. J. Neurochem. *88*, 246–256.

Andrade-Rozental, A.F., Rozental, R., Hopperstad, M.G., Wu, J.K., Vrionis, F.D., and Spray, D.C. (2000). Gap junctions: the "kiss of death" and the "kiss of life.". Brain Res. Brain Res. Rev. *32*, 308–315.

Arcuino, G., Lin, J.H., Takano, T., Liu, C., Jiang, L., Gao, Q., Kang, J., and Nedergaard, M. (2002). Intercellular calcium signaling mediated by point-source burst release of ATP. Proc. Natl. Acad. Sci. USA *99*, 9840–9845.

Ballerini, P., Rathbone, M.P., Di Iorio, P., Renzetti, A., Giuliani, P., D'Alimonte, I., Trubiani, O., Caciagli, F., and Ciccarelli, R. (1996). Rat astroglial P2Z ($P2X_7$) receptors regulate intracellular calcium and purine release. Neuroreport *7*, 2533–2537.

Becker, D.L., Evans, W.H., Green, C.R., and Warner, A. (1995). Functional analysis of amino acid sequences in connexin43 involved in intercellular communication through gap junctions. J. Cell Sci. *108*, 1455–1467.

Bennett, M.V., Contreras, J.E., Bukauskas, F.F., and Saez, J.C. (2003). New roles for astrocytes: gap junction hemichannels have something to communicate. Trends Neurosci. *26*, 610–617.

Berridge, M.J. (1995). Calcium signaling and cell proliferation. Bioessays *17*, 491–500.

Bittman, K., Owens, D.F., Kriegstein, A.R., and LoTurco, J.J. (1997). Cell coupling and uncoupling in the ventricular zone of developing neocortex. J. Neurosci. *17*, 7037–7044.

Braet, K., Vandamme, W., Martin, P.E., Evans, W.H., and Leybaert, L. (2003). Photoliberating inositol-1,4,5-trisphosphate triggers ATP release that is blocked by the connexin mimetic peptide gap 26. Cell Calcium *33*, 37–48.

Cai, L., Hayes, N.L., and Nowakowski, R.S. (1997). Synchrony of clonal cell proliferation and contiguity of clonally related cells: production of mosaicism in the ventricular zone of developing mouse neocortex. J. Neurosci. *17*, 2088–2100.

Catsicas, M., Bonness, V., Becker, D., and Mobbs, P. (1998). Spontaneous Ca^{2+} transients and their transmission in the developing chick retina. Curr. Biol. *8*, 283–286.

Ciccarelli, R., Di Iorio, P., D'Alimonte, I., Giuliani, P., Florio, T., Caciagli, F., Middlemiss, P.J., and Rathbone, M.P. (2000). Cultured astrocyte proliferation induced by extracellular guanosine involves endogenous adenosine and is raised by the co-presence of microglia. Glia *29*, 202–211.

Contreras, J.E., Sanchez, H.A., Eugenin, E.A., Speidel, D., Theis, M., Willecke, K., Bukauskas, F.F., Bennett, M.V., and Saez, J.C. (2002). Metabolic inhibition induces opening of unapposed connexin 43 gap junction hemichannels and reduces gap junctional communication in cortical astrocytes in culture. Proc. Natl. Acad. Sci. USA *99*, 495–500.

Cotrina, M.L., Lin, J.H., Alves-Rodrigues, A., Liu, S., Li, J., Azmi-Ghadimi, H., Kang, J., Naus, C.C., and Nedergaard, M. (1998). Connexins regulate calcium signaling by controlling ATP release. Proc. Natl. Acad. Sci. USA *95*, 15735–15740.

Cusato, K., Bosco, A., Rozental, R., Guimaraes, C.A., Reese, B.E., Linden, R., and Spray, D.C. (2003). Gap junctions mediate bystander cell death in developing retina. J. Neurosci. *23*, 6413–6422.

DeVries, S.H., and Schwartz, E.A. (1992). Hemi-gap-junction channels in solitary horizontal cells of the catfish retina. J. Physiol. *445*, 201–230.

Fischer, A.J., and Reh, T.A. (2001). Muller glia are a potential source of neural regeneration in the postnatal chicken retina. Nat. Neurosci. *4*, 247–252.

Fischer, A.J., and Reh, T.A. (2003). Potential of Muller glia to become neurogenic retinal progenitor cells. Glia *43*, 70–76.

Franke, H., Krugel, U., and Illes, P. (1999). P2 receptor-mediated proliferative effects on astrocytes in vivo. Glia *28*, 190–200.

Gourine, A.V., Llaudet, E., Dale, N., and Spyer, K.M. (2005). Release of ATP in the ventral medulla during hypoxia in rats: role in hypoxic ventilatory response. J. Neurosci. *25*, 1211–1218.

Guthrie, P.B., Knappenberger, J., Segal, M., Bennett, M.V., Charles, A.C., and Kater, S.B. (1999). ATP released from astrocytes mediates glial calcium waves. J. Neurosci. *19*, 520–528.

Hofer, A., and Dermietzel, R. (1998). Visualization and functional blocking of gap junction hemichannels (connexons) with antibodies against external loop domains in astrocytes. Glia *24*, 141–154.

Ilia, M., and Jeffery, G. (1996). Delayed neurogenesis in the albino retina: evidence of a role for melanin in regulating the pace of cell generation. Brain Res. Dev. Brain Res. *95*, 176–183.

Ilia, M., and Jeffery, G. (2000). Retinal cell addition and rod production depend on early stages of ocular melanin synthesis. J. Comp. Neurol. *420*, 437–444.

Jeffery, G. (1997). The albino retina: an abnormality that provides

insight into normal retinal development. Trends Neurosci. *20*, 165–169.

Li, H., Liu, T.F., Lazrak, A., Peracchia, C., Goldberg, G.S., Lampe, P.D., and Johnson, R.G. (1996). Properties and regulation of gap junctional hemichannels in the plasma membranes of cultured cells. J. Cell Biol. *134*, 1019–1030.

Llaudet, E., Botting, N.P., Crayston, J.A., and Dale, N. (2003). A three-enzyme microelectrode sensor for detecting purine release from central nervous system. Biosens. Bioelectron. *18*, 43–52.

LoTurco, J.J., and Kriegstein, A.R. (1991). Clusters of coupled neuroblasts in embryonic neocortex. Science *252*, 563–566.

Milenkovic, I., Weick, M., Wiedemann, P., Reichenbach, A., and Bringmann, A. (2003). P2Y receptor-mediated stimulation of Muller glial cell DNA synthesis: dependence on EGF and PDGF receptor transactivation. Invest. Ophthalmol. Vis. Sci. *44*, 1211–1220.

Moll, V., Weick, M., Milenkovic, I., Kodal, H., Reichenbach, A., and Bringmann, A. (2002). P2Y receptor-mediated stimulation of Muller glial DNA synthesis. Invest. Ophthalmol. Vis. Sci. *43*, 766–773.

Morita, M., Higuchi, C., Moto, T., Kozuka, N., Susuki, J., Itofusa, R., Yamashita, J., and Kudo, Y. (2003). Dual regulation of calcium oscillation in astrocytes by growth factors and pro-inflammatory cytokines via the mitogen-activated protein kinase cascade. J. Neurosci. *23*, 10944–10952.

Neary, J.T., and Zhu, Q. (1994). Signaling by ATP receptors in astrocytes. Neuroreport *5*, 1617–1620.

Neary, J.T., Kang, Y., Bu, Y., Yu, E., Akong, K., and Peters, C.M. (1999). Mitogenic signaling by ATP/P2Y purinergic receptors in astrocytes: involvement of a calcium-independent protein kinase C, extracellular signal-regulated protein kinase pathway distinct from the phosphatidylinositol-specific phospholipase C/calcium pathway. J. Neurosci. *19*, 4211–4220.

Newman, E.A. (2001). Propagation of intercellular calcium waves in retinal astrocytes and Muller cells. J. Neurosci. *21*, 2215–2223.

Pearson, R., Catsicas, M., Becker, D.L., and Mobbs, P. (2002). Purinergic and muscarinic modulation of the cell cycle and Ca^{2+} signaling in the chick retinal ventricular zone. J. Neurosci. *22*, 7569–7579.

Pearson, R.A., Catsicas, M., Becker, D.L., Bayley, P., Luneborg, N.L., and Mobbs, P. (2004). Ca^{2+} signaling and gap junction coupling within and between pigment epithelium and neural retina in the developing chick. Eur. J. Neurosci. *19*, 2435–2445.

Peinado, A., Yuste, R., and Katz, L.C. (1993). Extensive dye coupling between rat neocortical neurons during the period of circuit formation. Neuron *10*, 103–114.

Rachel, R.A., Dolen, G., Hayes, N.L., Lu, A., Erskine, L., Nowakowski, R.S., and Mason, C.A. (2002). Spatiotemporal features of early neuronogenesis differ in wild-type and albino mouse retina. J. Neurosci. *22*, 4249–4263.

Rathbone, M.P., Middlemiss, P.J., Kim, J.K., Gysbers, J.W., DeForge, S.P., Smith, R.W., and Hughes, D.W. (1992). Adenosine and its nucleotides stimulate proliferation of chick astrocytes and human astrocytoma. cells. Neurosci. Res. *13*, 1–17.

Raymond, S.M., and Jackson, I.J. (1995). The retinal pigmented epithelium is required for development and maintenance of the mouse neural retina. Curr. Biol. *5*, 1286–1295.

Ryu, J.K., Choi, H.B., Hatori, K., Heisel, R.L., Pelech, S.L., McLarnon, J.G., and Kim, S.U. (2003). Adenosine triphosphate induces proliferation of human neural stem cells: Role of calcium and p70 ribosomal protein S6 kinase. J. Neurosci. Res. *72*, 352–362.

Stout, C., and Charles, A. (2003). Modulation of intercellular calcium signaling in astrocytes by extracellular calcium and magnesium. Glia *43*, 265–273.

Stout, C.E., Costantin, J.L., Naus, C.C., and Charles, A.C. (2002). Intercellular calcium signaling in astrocytes via ATP release through connexin hemichannels. J. Biol. Chem. *277*, 10482–10488.

Sugioka, M., Fukuda, Y., and Yamashita, M. (1996). Ca^{2+} responses to ATP via purinoceptors in the early embryonic chick retina. J. Physiol. *493*, 855–863.

Sugioka, M., Zhou, W.L., Hofmann, H.D., and Yamashita, M. (1999). Involvement of P2 purinoceptors in the regulation of DNA synthesis in the neural retina of chick embryo. Int. J. Dev. Neurosci. *17*, 135–144.

Syed, M.M., Lee, S., He, S., and Zhou, Z.J. (2004). Spontaneous waves in the ventricular zone of developing mammalian retina. J. Neurophysiol. *91*, 1999–2009.

Weissman, T.A., Riquelme, P.A., Ivic, L., Flint, A.C., and Kriegstein, A.R. (2004). Calcium waves propagate through radial glial cells and modulate proliferation in the developing neocortex. Neuron *43*, 647–661.

Yuste, R., Nelson, D.A., Rubin, W.W., and Katz, L.C. (1995). Neuronal domains in developing neocortex: mechanisms of coactivation. Neuron *14*, 7–17.